AIMS Medical Science

AIMS Medical Science, 13(1): 67–88.
DOI: 10.3934/medsci.2026006
Received: 31 October 2025
Revised: 09 March 2026
Accepted: 11 March 2026
Published: 25 March 2026

http://www.aimspress.com/journal/medicalScience

Research article

An innovative multidisciplinary approach to thyroid research: Profile of the morphofunctional basic capability of follicular cells

Olha Ryabukha[1,*] and Taras Lahotskyi[2]

[1] Department of Anatomy, Physiology and Pathology, Faculty of Medicine, Private Higher Educational Institution "Lviv Medical University", Lviv, Ukraine
[2] Department of Economic Cybernetics, Faculty of Economics, Ivan Franko National University of Lviv, Ukraine

* **Correspondence:** Email: olha.ryabukha@medinstytut.lviv.ua; Tel: +380984493318.

Abstract: This study aimed to evaluate the knowledge of the interdependence and mutual influence among components of the morphofunctional basic capability profile of follicular cells. In a 1-month experiment, 4 groups of male albino rats were involved: Group 1 (control)—in conditions of a standard vivarium diet; Group 2—in conditions of an iodine deficiency; Group 3—in conditions of a potentiated iodine deficiency; and Group 4—in conditions of hyperthyroidism. The shape of the cells, the contour and condition of their lateral membranes, the shape of the nuclei, the contour of the karyolemmata, and the condition of the central and marginal chromatin were analyzed using electron micrographs. The author's methods were applied. Additionally, a Pearson correlation analysis and the process of creating graphic correlation portraits were employed. The main significance of the normal functioning of follicular cells is played by associations of unaltered lateral membranes, oval nuclei, and fine-grained central and narrow, unfragmented, highly dense marginal chromatin with other components of the profile. The following associations support the functioning of follicular cells under unfavorable conditions: (1) in the case of iodine deficiency—cuboidal and prismatic cells, fine-grained and sparse central chromatin, and narrow and wide marginal chromatin with other components of the profile; (2) in potentiated iodine deficiency—highly wavy karyolemmata, fine-grained and sparse central chromatin, and narrow marginal chromatin with other components of the profile; and (3) in hyperthyroidism—cylindrical nuclei and dense central chromatin with other components of the profile. An analysis of the correlation portraits of the morphofunctional basic capability deepens our understanding of the characteristics of interrelationships and interdependencies between follicular cell components under euthyroidism, hypothyroidism, and hyperthyroidism. When thyroid homeostasis is disturbed, the functioning of

follicular cells occurs, taking changes in the primary functional balance, the formation of compensatory and adaptive mechanisms, and the attainment of a new state of functional balance into account.

Keywords: thyroid; follicular cell; cytophysiology; euthyroidism; hypothyroidism; hyperthyroidism; correlation analysis; correlation portrait

1. Introduction

Thyroid hormones play a crucial role in maintaining the body's physiological balance [1,2]. Hypothyroidism, most commonly caused by iodine deficiency, is the most widespread thyroid disorder [3]. It leads to both physical and cognitive impairments, as manifested through a wide range of clinical symptoms [4]. Another prevalent thyroid pathology is hyperthyroidism, in which an increased functional activity of the thyroid gland induces dysfunction in other endocrine organs [5,6] and leads to the associated pathology [7]. The significant prevalence of thyroid disorders [8–10] and the steady increase in their various nosological forms [11,12] are largely determined by the unique embryological, histological, and anatomical characteristics of the thyroid gland, as well as its high sensitivity to external factors [13–15]. Given the vital importance of the thyroid gland for overall homeostasis [16,17], studying the specific mechanisms of thyroid pathology [18] represents a major global medical and social challenge [19], the resolution of which—especially in the post-COVID era—requires a multidisciplinary approach [20–23]. This challenge can be addressed by re-examining the problem through in-depth research into the functioning of follicular cells [24]. The production of thyroid hormones is a complex, multilevel process that simultaneously involves hormone synthesis, secretion, capillary transport, and the energy supply necessary to sustain these activities [25]. Thus, investigating thyroid hormone production transcends the boundaries of any single medical discipline; consequently, mathematical modeling is a promising approach, as it allows researchers to reveal the interdependence of different phenomena and physiological states [26,27]. According to the general systems theory [28], the main goal in diagnosing the state of any system is to identify the relationships among its individual features, their combinations, and their connection to the overall system state. We regard the follicular cell as a complex, non-entropic system whose subsystems, or domains, can be viewed as profiles of capabilities. The proposed mathematical approach involves characterizing the cellular components within these domains under conditions of euthyroidism, hypothyroidism, and hyperthyroidism [29]. This approach can be applied in the development of diagnostic expert systems [30] to identify the causes of hormone production disorders and to formulate recommendations for their correction. Currently, there is a pressing need to explore integrative approaches to understand the functioning of follicular cells. One promising method for this research is analyzing their morphofunctional basic capability profile. The aim of the article was achieved.

2. Materials and methods

2.1. Study design and methods

Forty nonlinear male albino rats, with an initial body weight of 140–160 g, were housed under standard vivarium conditions for 30 days in the summer. They received their food mixture once a day in the morning; access to distilled water was freely available. All nutrients were supplied in the amounts recommended for animals of this species and weight.

Rats in Group 1 (control) were fed standard chow. Rats in groups 2, 3, and 4 consumed a semi-synthetic, isocaloric starch-casein diet (see Table 1). The protein source was acid casein (Lactalis, Ukraine), and carbohydrates were provided by corn starch (Intercorn CPI, Ukraine). Fats, phytosterols, polyunsaturated fatty acids, and α-tocopheryl acetate were supplied via organic cold-pressed unrefined sunflower oil (Ecorod, Ukraine) at a dose of 5.0 ml per 100 g of dry feed. Water-soluble vitamins were dissolved in distilled water and added to the diet immediately before preparation. Essential macro- and microelements were supplied with the classic salt mixture No. 12 by J.H. Jones & C. Foster [31], from which potassium iodide was removed.

Table 1. Composition of the semi-synthetic isocaloric starch-casein diet.

Ingredients	Weigh (g)	Proteins (g)	Fats (g)	Carbohydrates (g)
Casein	20.3	17.9	0.3	null
Corn starch	64.2	0.64	null	55.36
Sunflower oil	11.5	null	11.48	null
Salt mixture 12*	4.0	null	null	null
Total	100.0	18.54	11.78	55.36

Note: * Under the conditions of the experiment, potassium iodide was removed.

Table 2. Experimental study organization.

Group	Condition	Background iodine content	Substance to change the condition, dose
1 N = 10	euthyroidism	did not determine	absent
2 N = 10	iodine deficiency	13–15 μg/kg body weight (equivalent to 1.6–1.8 μg/rat/day)	absent
3 N = 10	potentiated iodine deficiency	13–15 μg/kg body weight (equivalent to 1.6–1.8 μg/rat/day)	Thiamazole, 3 mg/kg body weight
4 N = 10	hyperthyroidism	13–15 μg/kg body weight (equivalent to 1.6–1.8 μg/rat/day)	Thyroidin, 15 mg/100 g body weight

Rats in Group 2 were in hypothyroid conditions. The drug *Mercazolil*, Pharm Comp "Zdorovye" Ukraine (INN: Thiamazole), at a dose of 3 mg/kg body weight, was added to the iodine-deficient diet to induce a potentiated iodine deficiency (Group 3). Since the current approach to modeling biomedical experiments involves the use of natural substances [32], desiccated thyroid extract was used as a dietary

supplement to induce hyperthyroidism. Thyroidin substance, Uralbiopharm JSC, Russia (INN: Thyroidin) [33], was administered at a dose of 15 mg/100 g body weight (Group 4). Histomorphological studies determined the doses. The organization of the study is presented in Table 2.

After the experimental phase, the rats were decapitated under ether anesthesia, and their thyroid glands removed and carefully separated from the connective tissue. The samples were prepared by the routine method; an LKB 8800 ultramicrotome (Sweden) and a Selmi TEM-100-01 electron microscope (Ukraine) were used.

The study focused on electron micrographs of ultrathin (4–6 μm) sections of the thyroid gland. The morphological pattern of experimental thyroid tissue was described based on the classical works of Petrovici & Lupulescu [34,35] and others. The obtained results served as the basis for the author's method [36]. This method involves clustering ultrastructural components within a selected domain of cellular function. The following integrative characteristics were selected as key components of the basic morphofunctional profile of follicular cells: cell shape, contour of lateral membranes, presence or absence of degenerative alterations of cell membranes, nuclear shape, contour of the nuclear membrane, and chromatin condition. The ranked components of the profile of the morphofunctional basic capability of follicular cells are presented in Table 3.

Table 3. The morphofunctional basic capability profile of the follicular cell.

Cluster	Component of profile	Morphological status	Symbol
Cell	shape cell	flattened	A1
		cuboidal	A2
		prismatical	A3
	Lateral membrane	moderately wavy	A4
		highly wavy	A5
		unaltered	A6
		degeneratively altered	A7
Nucleus	shape nucleus	rounded	C1
		oval	C2
		cylindrical	C3
		irregular	C4
	Karyolemma	moderately wavy	C5
		highly wavy	C6
	Central chromatin	homogeneous	C7
		fine-grained	C8
		lumpy	C9
		sparse	C10
		dense	C11
		spotted (unevenly dense)	C12
	Marginal chromatin	narrow, fragmented, highly dense	C13
		narrow, unfragmented, highly dense	C14
		wide, highly dense	C15

To describe the variety of chromatin visual types, we grouped them into two categories: (1) general appearance—homogeneous, fine-grained, or lumpy; and (2) structural characteristics—sparse, dense, highly dense, or spotted.

To mathematically validate the conclusions of the study, the linguistic descriptions were converted into numerical equivalents using another author's method [37]. The method is based on the concept of fuzzy logic about the possibility of such a transformation [38]. The electron microscopic pattern is compared with two controls: the norm and uncorrected experimental pathology. According to the principle of phase interval, the electron microscopic pattern is compared with two controls: the norm and the uncorrected experimental pathology. Then, it is evaluated on a 5-point scale (0 to 4 points) [36].

2.2. Statistical analysis

A bivariate correlation analysis was performed to identify statistically significant associations between the follicular cell components. Typically, a multivariate analysis requires large sample sizes, strict assumptions about variable distributions, and a clearly specified model. Cluster analysis methods aim to group observations into homogeneous categories based on their similarity. A correlation analysis was selected as the most appropriate method because it offers a simple and interpretable way to identify and quantify relationships among follicular cell components, thus enabling the reliable and transparent determination of statistically significant pairwise correlations. The process of studying the relationship between follicular cell components involved transforming qualitative and binary data (linguistic characteristics of follicular cells) into quantitative parameters by evaluating the arithmetic mean (M) and Pearson's correlation coefficients (r). A statistical analysis was performed using IBM SPSS Statistics, version 31 (IBM, Chicago, IL), and Microsoft Excel. The obtained r-coefficients were interpreted according to the Chaddock scale [39]. We deemed the correlations to be the most significant when they were very strong ($0.91 \leq r \leq 1.00$) and strong ($0.71 \leq r \leq 0.90$). Additionally, we took marked correlations ($0.51 \leq r \leq 0.70$) and moderate correlations ($0.31 \leq r \leq 0.50$) into account for additional analyses.

The observed correlations were graphically represented as correlation portraits [37]. The to interpret correlation portraits was the knowledge of classical cytophysiology regarding the functions of cellular ultrastructures and their electron-microscopic characteristics [40–42].

2.3. Ethics approval of research

The Bioethics Committee of the Private Higher Educational Institution "Lviv Medical University" approved the experimental design. During observation and euthanasia, bioethical principles were observed in accordance with the European Convention for the Protection of Vertebrate Animals Used for Experimental and Other Scientific Purposes (Strasbourg, 1986), and Directive 2010/63/EU of the European Parliament and of the Council of 22 September 2010.

3. Results and discussion

The results of the pairwise Pearson correlation analysis between the components of the morphofunctional basic capability profile of follicular cells are presented in Figures 1, 2, 3, and 4.

We refer to the “actual” components of the correlation portrait as the components of the implementing cells of the studied domain, between which associations were identified.

3.1. A descriptive analysis of electron micrographs of follicular cells in intact nonlinear male albino rats (*Group 1*)

Follicular cells are cuboidal. Their lateral membranes are uneven, with protrusions and depressions. The nuclei are usually rounded and located in the basal part of the cells, though they are sometimes oval. The contours of the karyolemmata are uneven due to the presence of protrusions of various sizes and shapes. Central chromatin is fine-grained and homogeneous. Marginal chromatin is narrow, unfragmented, and highly dense.

	A1	A2	A3	A4	A5	A6	A7	C1	C2	C3	C4	C5	C6	C7	C8	C9	C10	C11	C12	C13	C14	C15
A1																						
A2				0.645	-0.612	-0.408		0.667	-0.612			-0.667	0.873	0.612	-0.408			-0.408			-0.408	
A3																						
A4		0.645			-0.791	-0.791		0.645	-0.791			-0.645	0.845	0.791	-0.791			0.000			-0.791	
A5		-0.612		-0.791		0.250		-0.408	1.000			0.408	-0.535	-1.000	0.250			0.250			0.250	
A6		-0.408		-0.791	0.250			-0.612	0.250			0.612	-0.802	-0.250	1.000			-0.250			1.000	
A7																						
C1		0.667		0.645	-0.408	-0.612			-0.408			-1.000	0.764	0.408	-0.612			-0.612			-0.612	
C2		-0.612		-0.791	1.000	0.250		-0.408				0.408	-0.535	-1.000	0.250			0.250			0.250	
C3								0.000														
C4																						
C5		-0.667		-0.645	0.408	0.612		-1.000	0.408				-0.764	-0.408	0.612			0.612			0.612	
C6		0.873		0.845	-0.535	-0.802		0.764	-0.535			-0.764		0.535	-0.802			-0.134			-0.802	
C7		0.612		0.791	-1.000	-0.250		0.408	-1.000			-0.408	0.535		-0.250			-0.250			-0.250	
C8		-0.408		-0.791	0.250	1.000		-0.612	0.250			0.612	-0.802	-0.250				-0.250			1.000	
C9																						
C10																						
C11		-0.408		0.000	0.250	-0.250		-0.612	0.250			0.612	-0.134	-0.250	-0.250						-0.250	
C12																						
C13																						
C14		-0.408		-0.791	0.250	1.000		-0.612	0.250			0.612	-0.802	-0.250	1.000			-0.250				
C15																						

Very strong association
Strong association
Marked association
Moderate association

Figure 1. List of *r*-coefficients representing interrelationships between components of the morphofunctional basic capability profile of follicular cells under normal dietary iodine intake. Note: See the meaning of the symbols in Table 3.

	A1	A2	A3	A4	A5	A6	A7	C1	C2	C3	C4	C5	C6	C7	C8	C9	C10	C11	C12	C13	C14	C15
A1																						
A2			0.845	0.873		0.535	0.873	0.423	0.134		0.535	0.535		0.327	-0.218		-0.218	0.000	0.429	0.873		0.873
A3		0.845		0.645		0.791	0.645	0.500	0.000		0.000	0.000		0.000	0.000		0.000	0.500	0.423	0.645		0.645
A4		0.873	0.645			0.612	1.000	0.000	0.408		0.612	0.612		0.167	0.167		0.167	0.000	0.764	1.000		1.000
A5																						
A6		0.535	0.791	0.612			0.612	0.000	0.250		-0.250	-0.250		-0.408	0.612		0.612	0.791	0.802	0.612		0.612
A7		0.873	0.645	1.000		0.612		0.000	0.408		0.612	0.612		0.167	0.167		0.167	0.000	0.764	1.000		1.000
C1		0.423	0.500	0.000		0.000	0.000		-0.791		0.000	0.000		0.645	-0.645		-0.645	0.000	-0.423	0.000		0.000
C2		0.134	0.000	0.408		0.250	0.408	-0.791			0.250	0.250		-0.612	0.408		0.408	0.000	0.535	0.408		0.408
C3																						
C4		0.535	0.000	0.612		-0.250	0.612	0.000	0.250			1.000		0.612	-0.408		-0.408	-0.791	0.134	0.612		0.612
C5		0.535	0.000	0.612		-0.250	0.612	0.000	0.250		1.000			0.612	-0.408		-0.408	-0.791	0.134	0.612		0.612
C6																						
C7		0.327	0.000	0.167		-0.408	0.167	0.645	-0.612		0.612	0.612			-0.667		-0.667	-0.645	-0.327	0.167		0.167
C8		-0.218	0.000	0.167		0.612	0.167	-0.645	0.408		-0.408	-0.408		-0.667			1.000	0.645	0.764	0.167		0.167
C9																						
C10		-0.218	0.000	0.167		0.612	0.167	-0.645	0.408		-0.408	-0.408		-0.667	1.000			0.645	0.764	0.167		0.167
C11		0.000	0.500	0.000		0.791	0.000	0.000	0.000		-0.791	-0.791		-0.645	0.645		0.645		0.423	0.000		0.000
C12		0.429	0.423	0.764		0.802	0.764	-0.423	0.535		0.134	0.134		-0.327	0.764		0.764	0.423		0.764		0.764
C13		0.873	0.645	1.000		0.612	1.000	0.000	0.408		0.612	0.612		0.167	0.167		0.167	0.000	0.764			1.000
C14																						
C15		0.873	0.645	1.000		0.612	1.000	0.000	0.408		0.612	0.612		0.167	0.167		0.167	0.000	0.764	1.000		

Very strong association Strong association
Marked association Moderate association

Figure 2. List of *r*-coefficients representing interrelationships between components of the morphofunctional basic capability profile of follicular cells under iodine deficiency. Note: See the meaning of the symbols in Table 3.

	A1	A2	A3	A4	A5	A6	A7	C1	C2	C3	C4	C5	C6	C7	C8	C9	C10	C11	C12	C13	C14	C15
A1																						
A2																						
A3					-1.000		1.000	0.612					-0.250	-0.791	-0.250	0.000	0.250	-0.375	-0.535	0.250	-0.802	
A4																						
A5			-1.000				-1.000	-0.612					0.250	0.791	0.250	0.000	-0.250	0.375	0.535	-0.250	0.802	
A6																						
A7			1.000		-1.000			0.612					-0.250	-0.791	-0.250	0.000	0.250	-0.375	-0.535	0.250	-0.802	
C1			0.612		-0.612		0.612						-0.408	0.000	-0.408	-0.645	0.408	-0.102	-0.873	0.408	-0.218	
C2																						
C3																						
C4																						
C5																						
C6			-0.250		0.250		-0.250	-0.408						0.000	1.000	0.791	-1.000	0.875	0.802	-1.000	0.535	
C7			-0.791		0.791		-0.791	0.000					0.000		0.000	-0.500	0.000	0.395	0.000	0.000	0.845	
C8			-0.250		0.250		-0.250	-0.408					1.000	0.000		0.791	-1.000	0.875	0.802	-1.000	0.535	
C9			0.000		0.000		0.000	-0.645					0.791	-0.500	0.791		-0.791	0.395	0.845	-0.791	0.000	
C10			0.250		-0.250		0.250	0.408					-1.000	0.000	-1.000	-0.791		-0.875	-0.802	1.000	-0.535	
C11			-0.375		0.375		-0.375	-0.102					0.875	0.395	0.875	0.395	-0.875		0.535	-0.875	0.802	
C12			-0.535		0.535		-0.535	-0.873					0.802	0.000	0.802	0.845	-0.802	0.535		-0.802	0.429	
C13			0.250		-0.250		0.250	0.408					-1.000	0.000	-1.000	-0.791	1.000	-0.875	-0.802		-0.535	
C14			-0.802		0.802		-0.802	-0.218					0.535	0.845	0.535	0.000	-0.535	0.802	0.429	-0.535		
C15																						

Very strong association
Strong association
Marked association
Moderate association

Figure 3. List of *r*-coefficients representing interrelationships between components of the morphofunctional basic capability profile of follicular cells under potentiated iodine deficiency. Note: See the meaning of the symbols in Table 3.

	A1	A2	A3	A4	A5	A6	A7	C1	C2	C3	C4	C5	C6	C7	C8	C9	C10	C11	C12	C13	C14	C15
A1					-0.250	-0.686	-0.612			0.612		-0.250	-0.612			0.612		-0.250	0.791		0.612	-0.612
A2																						
A3																						
A4																						
A5	-0.250					0.294	0.408			-0.408		-0.250	0.408			0.612		-0.250	0.000		-0.408	0.408
A6	-0.686				0.294		-0.080			0.080		0.784	-0.080			-0.320		0.784	-0.930		0.080	-0.080
A7	-0.612				0.408	-0.080				-1.000		-0.612	1.000			-0.167		-0.612	0.000		-1.000	1.000
C1																						
C2																						
C3	0.612				-0.408	0.080	-1.000					0.612	-1.000			0.167		0.612	0.000		1.000	-1.000
C4																						
C5	-0.250				-0.250	0.784	-0.612			0.612			-0.612			-0.408		1.000	-0.791		0.612	-0.612
C6	-0.612				0.408	-0.080	1.000			-1.000		-0.612				-0.167		-0.612	0.000		-1.000	1.000
C7																						
C8																						
C9	0.612				0.612	-0.320	-0.167			0.167		-0.408	-0.167					-0.408	0.645		0.167	-0.167
C10																						
C11	-0.250				-0.250	0.784	-0.612			0.612		1.000	-0.612			-0.408			-0.791		0.612	-0.612
C12	0.791				0.000	-0.930	0.000			0.000		-0.791	0.000			0.645		-0.791			0.000	0.000
C13																						
C14	0.612				-0.408	0.080	-1.000			1.000		0.612	-1.000			0.167		0.612	0.000			-1.000
C15	-0.612				0.408	-0.080	1.000			-1.000		-0.612	1.000			-0.167		-0.612	0.000		-1.000	

Very strong association
Strong association
Marked association
Moderate association

Figure 4. List of *r*-coefficients representing interrelationships between components of the morphofunctional basic capability profile of follicular cells under hyperthyroidism. Note: See the meaning of the symbols in Table 3.

3.1.1. Analysis of the correlation portrait structure of the morphofunctional basic capability profile of follicular cells in intact nonlinear male albino rats (Group 1)

The "actual" components of the correlation portrait are A2, A4, A5, A6, C1, C2, C5, C6, C7, C8, and C14 (see Figure 5), between which the following correlations are observed: very strong —7 (of which 3 are negative); strong—13 (of which 9 are negative); marked—19 (of which 10 are negative); moderate—10 (of which 7 are negative). The moderate predominance of negative correlations in the architectonics of the portrait (59.2% versus 40.8%) gives the structure an overall balance, which is determined by its ability to change against the background of stability, which is provided by 8 very strong and strong positive associations.

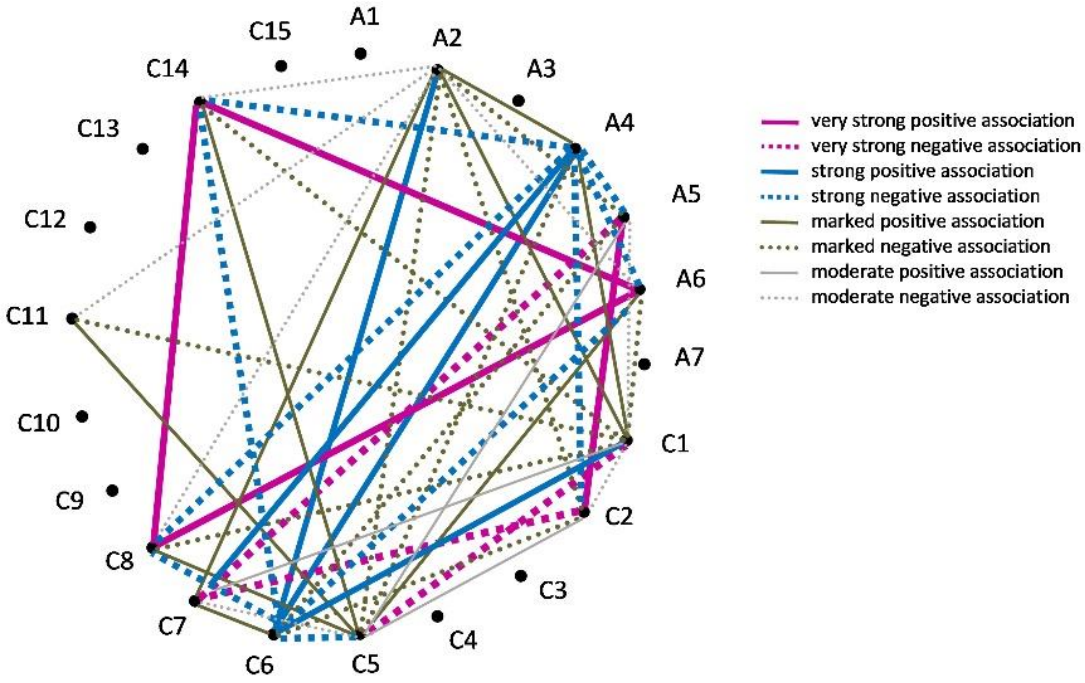

Figure 5. Correlation portrait of the morphofunctional basic capability of follicular cells under normal dietary iodine intake.

A set of associations of varying strengths and directions between the profile components indicates the presence of favorable conditions for thyroid hormone production. The most important among them are the very strong positive associations of unaltered lateral membranes (A6) and fine-grained central chromatin (C8), as well as narrow, unfragmented, highly dense marginal chromatin (C14); moreover, there is a marked association in the same direction between follicular cells of cuboidal shape (A2) and moderately wavy lateral membranes (A4). Other significant correlations in this group include the following: marked positive associations between A2 and rounded nuclei (C1) and homogeneous central chromatin (C7); associations between A4 and C1; associations between unaltered lateral membranes (A6) and moderately wavy karyolemmata (C5); and associations between C5 and C8 and C14. Moreover, this category of correlations includes the following group of moderate associations: (1) moderate positive – between rounded nuclei (C1) and homogeneous central chromatin (C7), and between oval nuclei (C2) and moderately wavy karyolemmata (C5); (2) moderate negative – between

cells of cuboidal shape (A2) and dense central chromatin (C11), as well as narrow, unfragmented, highly dense marginal chromatin (C14).

A key feature of the portrait is the examination of the adaptive mechanisms of follicular cells. These are the connections between the components of the profile, which are promising to understand the fundamental foundations of cytophysiology. We include a large group of positive associations, among which are the following: a very strong association between highly wavy lateral membranes (A5) and oval nuclei (C2); a strong association between cells of cuboidal shape (A2) and highly wavy karyolemmata (C6); a marked association between C6 and homogeneous central chromatin (C7); and moderate associations involving moderately wavy karyolemmata (C5), A5, and C2. At the same time, most adaptation mechanisms are represented by negative correlations, including the following: a very strong association between highly wavy lateral membranes (A5) and homogeneous central chromatin (C7); an association between rounded nuclei (C1) and C5; a strong association between highly wavy karyolemmata (C6) and unaltered lateral membranes (A6); marked associations between C1 and dense central chromatin (C11), and narrow, unfragmented, highly dense marginal chromatin (C14); and moderate associations between cubic-shaped cells (A2), unaltered lateral membranes (A6), and fine-grained central chromatin (C8), as well as between rounded (C1) and oval (C2) nuclei. In our opinion, the observed correlations help maintain the stable functioning of hormone-producing cells.

Thus, under standard vivarium feeding conditions, the following profile components are of great importance for the normal hormone-producing activity of follicular cells: unaltered lateral membranes, oval-shaped nuclei, fine-grained central chromatin, and narrow, unfragmented, highly dense marginal chromatin. The connection between cuboidal cells and moderately wavy lateral membranes appears to be less functionally significant. In contrast, correlations between cells with unaltered or highly wavy lateral membranes and other profile components demonstrate how follicular cells adapt to changing conditions.

3.2. A descriptive analysis of electron micrographs of follicular cells in nonlinear male albino rats under conditions of iodine deficiency (*Group 2*)

The follicular cells are cylindrical, and the nuclei of most cells are oval and located in the basal part of the cell. The contours of the nuclei are moderately wavy. Central chromatin appears as small, diffusely arranged grains of a moderate electron density. Larger areas of rarefied chromatin are found next to smaller regions of compacted chromatin, thus defining the motley structure of the nucleus. Marginal chromatin is often weakly expressed. Irregularly shaped nuclei with wide, highly compacted, unfragmented marginal chromatin may be observed. The phenomena of cell disintegration are present to a slight or moderate degree. The general morphological pattern indicates a reduced functional activity.

3.2.1. Analysis of the correlation portrait structure of the morphofunctional basic capability profile of follicular cells in nonlinear male albino rats under conditions of iodine deficiency (Group 2)

The “actual” components of the correlation portrait are A2, A3, A4, A7, C4, C5, C8, C10, C13, and C15 (see Figure 6), between which the following correlations were observed: very strong—8 (all positive); strong—17 (3 of them are negative); marked—33 (6 of them aqre negative); and moderate—

20 (7 of them are negative). The portrait's architectonics are characterized by symmetry. Its rigidity stems from the significant predominance of positive associations (79.5%) over negative ones, thus providing it with stability under adverse conditions. A very strong positive association between moderately wavy lateral membranes (A4) and degeneratively altered lateral membranes (A7), and a strong positive association between A7 and cuboidal cells (A2), indicate that the functioning of follicular cells occurs against the background of thyroid homeostasis disturbance. Additional signs of functional load include a very strong positive association between moderately wavy karyolemmata (C5) and irregularly shaped nuclei (C4), as well as marked positive associations between A2 and C4, between cells of prismatic shape (A3) and degeneratively altered lateral membranes (A7), and between A7 and C4. Additionally, this is indicated by a marked positive association between homogeneous (C7) and dense (C11) central chromatin.

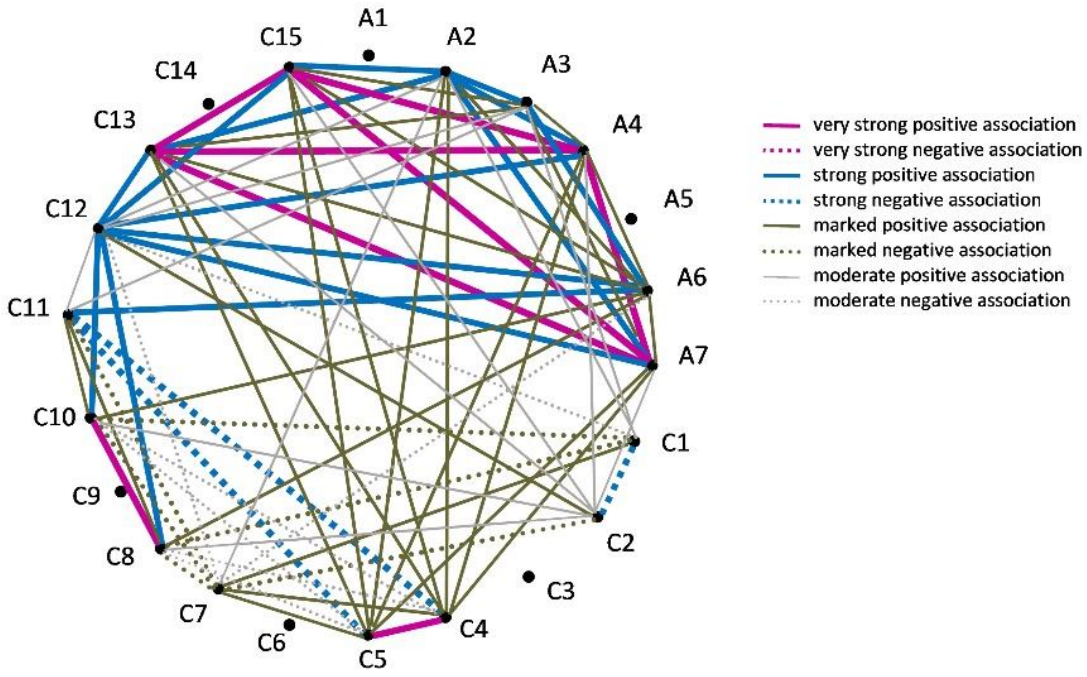

Figure 6. Correlation portrait of the morphofunctional basic capability of follicular cells under iodine deficiency.

At the same time, we identified correlations that suggest mechanisms by which follicular cells adapt to activity under adverse conditions. The main ones we consider have a very strong positive association between the lateral cell membranes that show signs of degeneration (A7) and narrow, fragmented, highly dense, and wide, highly dense marginal chromatin (C13 and C15, respectively). Additionally, adaptation mechanisms consist of a set of high, mostly positive associations. These include the following connections: between C13 and C15 and spotted (unevenly compacted) central chromatin (C12); between follicular cells of cuboidal and prismatic shape (A2 and A3, respectively); between A2, narrow, fragmented, highly compacted (C13), and wide, highly dense (C15) marginal chromatin; between A6, dense (C11), and spotted (C12) central chromatin; and connections between C12, fine-grained (C8), and sparse (C10) central chromatin.

Information about sufficient thyroid hormone production is important, as supported by the varying strengths and directions of correlations between the components of the profile. These include very strong positive associations between moderately wavy lateral membranes (A4), narrow, fragmented, highly dense (C13), and wide, highly dense (C15) marginal chromatin, as well as between fine-grained (C8) and sparse (C10) central chromatin. Additionally, there are strong positive associations between cuboidal cells (A2) and A4, as well as between prismatic cells (A3) and unaltered lateral membranes (A6). This group of correlations also includes marked positive associations as follows: between A4 and A6; between A6, fine-grained (C8), sparse (C10) central chromatin, narrow, fragmented, highly dense (C13), and wide, highly dense (C15) marginal chromatin; and moderate positive associations between cells of cuboidal shape (A2) and rounded nuclei (C1), and between oval nuclei (C2) and moderately wavy lateral membranes (A4), C8, C10, C13, and C15.

Thus, the correlations between lateral cell membranes with signs of degeneration, irregularly shaped nuclei, dense and unevenly dense (spotted) central chromatin, and other components of the profile indicate a change of functional balance in follicular cells in hypothyroidism caused by a dietary iodine deficiency. The main mechanisms by which follicular cells adapt to functioning under unfavorable conditions involve specific correlations between cubic-shaped cells, prism-shaped cells, highly condensed marginal chromatin of varying widths (either narrow or wide), and various structural components of the profile. Evidence of the preserved functional activity in follicular cells is demonstrated by characteristic associations among moderately wavy or unaltered lateral membranes, cubic-shaped cells, moderately wavy karyolemmata, and central chromatin that appears homogeneous, fine-grained, and sparse.

3.3. A descriptive analysis of electron micrographs of follicular cells in nonlinear male albino rats under conditions of potentiated iodine deficiency (*Group 3*)

The follicular epithelium consists of tall, cylindrical cells. Occasionally, cells with destroyed apical membranes and cytoplasm that enter the follicle cavity are observed. Some follicular cells have apical membranes that protrude into the follicle cavity in the form of a cushion, where vacuoles are formed. The structure and degree of electron density of the vacuole contents are similar to those of the intrafollicular colloid. The nuclei of follicular cells are rounded and located in the basal part of the cells. They have wavy, clear contours. The central chromatin appears as small lumps; against the background of its predominantly homogeneous structure, it often forms cloud-like condensations. The marginal chromatin is narrow and occasionally fragmented. The overall morphological profile indicates a reduced level of hormonal activity.

3.3.1. Analysis of the correlation portrait structure of the morphofunctional basic capability profile of follicular cells in nonlinear male albino rats under conditions of potentiated iodine deficiency (Group 3)

The “actual” components of the correlation portrait are A3, A5, A7, C1, C6, C7, C8, C9, C10, C11, C12, C13, and C14 (see Figure 7), between which the following associations were observed: very strong—9 (6 of them are negative); strong—22 (11 of them are negative); marked—12 (6 of them are negative); and moderate—11 (5 of them are negative). A certain asymmetry, with a predominance of chromatin correlations, characterizes the architectonics of the portrait. Meanwhile, the nearly uniform

distribution of correlations into very high and high categories by strength and into positive and negative categories by direction indicates the system's ability to maintain the equilibrium, adapt to changes, and continue its activity under the adverse conditions of a potentiated iodine deficiency.

A group of positive and negative correlations with very high and high values indicates disorders of the functional activity of follicular cells. A very strong positive associations is observed between prism-shaped cells (A3) and cells with degeneratively altered membranes (A7). Strong associations of the same direction include the connections between highly wavy karyolemmata (C6), lumpy chromatin (C9), and spotted central chromatin (C12), as well as the connection between C12 and C9. Negative correlations, which are signs of impaired hormone production, include a very strong association between fine-grained central chromatin (C8) and sparse central chromatin (C10), as well as the following strong associations: between C10 and C9; dense central chromatin (C11) and narrow, fragmented, highly dense marginal chromatin (C13); and the connections between C13 and both C9 and C11.

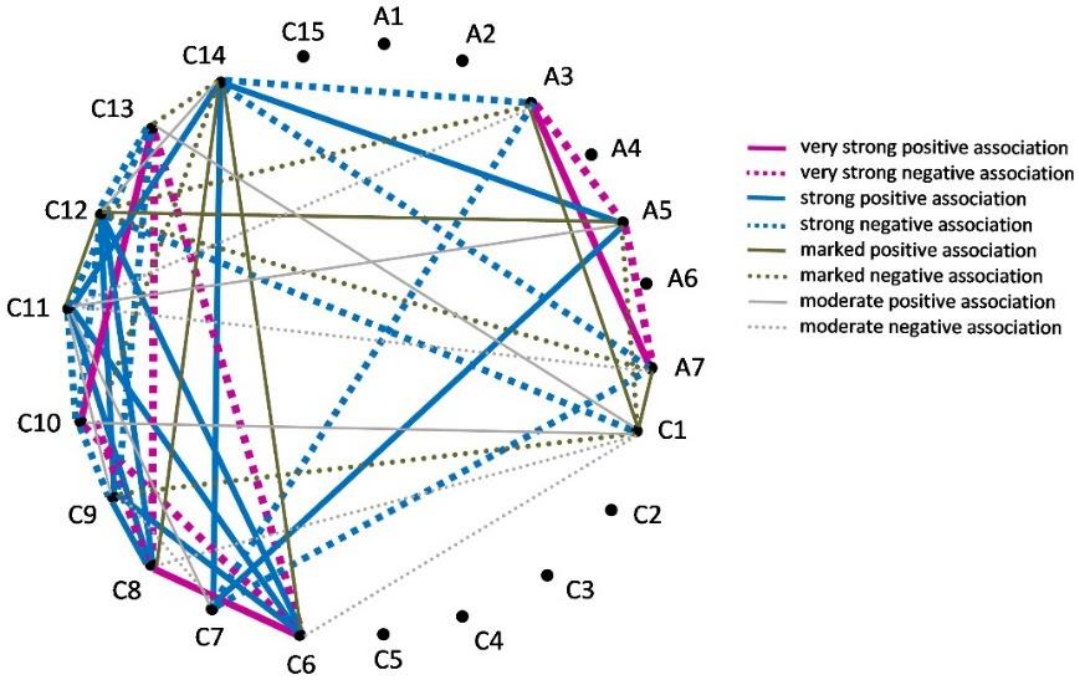

Figure 7. Correlation portrait of the morphofunctional basic capability of follicular cells under potentiated iodine deficiency.

At the same time, a complex of correlations that differ in direction and strength indicates mechanisms that promote thyroid hormone production. In particular, the mechanisms of activation of follicular cells under conditions of a high functional load include the following: a very strong positive association between highly wavy karyolemmata (C6) and fine-grained central chromatin (C8); strong positive associations between highly wavy lateral membranes (A5), homogeneous central chromatin (C7), and narrow, unfragmented, highly dense marginal chromatin (C14); and relationships of such strength and direction between fine-grained (C8), dense (C11), and spotted (C12) central chromatin, as well as between C11 and C14.

An important set of negative associations also points to mechanisms by which follicular cells adapt to functions under conditions of disturbed thyroid homeostasis. In particular, we observed the following: very strong associations between highly wavy karyolemmata (C6), sparse central chromatin (C10), narrow, fragmented, highly dense marginal chromatin (C13); and strong associations between C13 and spotted central chromatin (C12), and between narrow, unfragmented, highly dense marginal chromatin (C14), prism-shaped cells (A3), and degeneratively altered lateral membranes (A7). The important components for forming correlations were A3, A5, A7, C1, C6, C9, C11, C13, and C14.

Positive and negative correlations of varying strengths provide evidence of the continuation of the hormone-producing activity of follicular cells under adverse conditions of potentiated iodine deprivation. An important aspect is the following positive associations: (1) a very strong association between prism-shaped cells (A3) and degeneratively altered lateral membranes (A7), and between sparse central chromatin (C10) and narrow, fragmented, highly dense marginal chromatin (C13); (2) a strong association between homogeneous central chromatin (C7) and narrow, unfragmented, highly dense marginal chromatin (C14), and between fine-grained chromatin (C8) and lumpy central chromatin (C9); (3) a marked association between rounded nuclei (C1) and prism-shaped cells (A3); (4) a moderate association between rounded nuclei (C1) and C13; and (5) the very strong negative association between highly wavy lateral membranes (A5) and A3 and A7. Moreover, the marked positive association between rounded nuclei (C1) and A3 was favorable, as well as a moderate association between C1 and narrow, fragmented, highly dense marginal chromatin (C13).

Thus, in potentiated hypothyroidism—caused by iodine deficiency and aggravated by the intake of thyrostatic drugs—a correlation exists between prism-shaped cells and cells with degeneratively altered lateral membranes, as well as between lumpy and spotted chromatin located near the center of the nucleus, thus indicating a disruption in hormone production. Under these conditions, the range of adaptive mechanisms expands. The main mechanisms are the connections between the nuclear characteristics, such as its rounded shape, highly wavy karyolemma, fine-grained and sparse central chromatin, and narrow, fragmented and unfragmented, highly dense marginal chromatin. The normal functioning of follicular cells is primarily supported by chromatin association.

3.4. A descriptive analysis of electron micrographs of follicular cells in nonlinear male albino rats under conditions of drug-induced hyperthyroidism (*Group 4*)

The follicular epithelium is composed of flattened cells, and their lateral membranes are mostly highly wavy. The intrafollicular colloid is dense. The nuclei are elongated (cylindrical) and located in the basal part of the cells. The contours of the karyolemmata are clear and predominantly highly wavy. The central chromatin is dense and spotted. The marginal chromatin is narrow, unfragmented, and highly dense. The overall morphological pattern indicates an increased hormonal activity. The observed morphological pattern is indicative of elevated hormonal activity.

3.4.1. Analysis of the correlation portrait structure of the morphofunctional basic capability profile of follicular cells in nonlinear male albino rats under conditions of drug-induced hyperthyroidism (Group 4)

The “actual” components of the correlation portrait are A6, A7, C3, C5, C6, C11, C12, C14, and C15 (see Figure 8), between which the following associations were observed: very strong—12 (7 of

them are negative); strong—5 (2 of them are negative); marked—19 (10 of them are negative); and moderate—8 (5 of them are negative). The portrait architectonics are quite symmetrical. A significant percentage (40%) of nuclear component associations is due to chromatin associations. The presence of 17 strong and very strong associations out of 44 significant correlations, as well as their nearly even distribution between positive (20) and negative (24) ones, indicates the system's stability and ability to adapt to changes. Functional overload in follicular cells under hyperthyroidism is evidenced by a very strong positive association between highly wavy karyolemmata (C6) and degeneratively altered lateral membranes (A7), as well as with wide marginal chromatin (C15). Additionally, there is a strong negative correlation between A7 and narrow, unfragmented, and highly dense marginal chromatin (C14). The marked positive correlation between lumpy chromatin (C9) and spotted central chromatin (C12), as well as with highly wavy lateral membranes (A5), suggests unfavorable conditions for follicular cell function. This is further supported by negative associations of the same strength between flattened cells (A1) and unaltered lateral membranes (A6), and between degeneratively altered lateral membranes (A7) and moderately wavy karyolemmata (C5).

At the same time, follicular cells have sufficient reserves for physiological hormone production under conditions of hyperthyroidism, which is indicated by the following: a very strong negative association between the unaltered lateral membranes (A6) and spotted central chromatin (C12); a strong positive association between A6 and moderately wavy karyolemmata (C5); and marked and moderate associations among profile components. Marked associations include the following: positive associations between cells of flattened shape (A1), narrow, unfragmented, highly dense marginal chromatin (C14), and cylindrical nuclei (C3); between moderately wavy karyolemmata (C5) and C3 and C14; and negative correlations of the same strength between C5, highly wavy karyolemmata (C6) and wide marginal chromatin (C15). Instead, moderate correlations are primarily negative connections. For example, there is a correlation between C3 and highly wavy lateral membranes (A5), as well as between unaltered lateral membranes (A6) and lumpy central chromatin (C9).

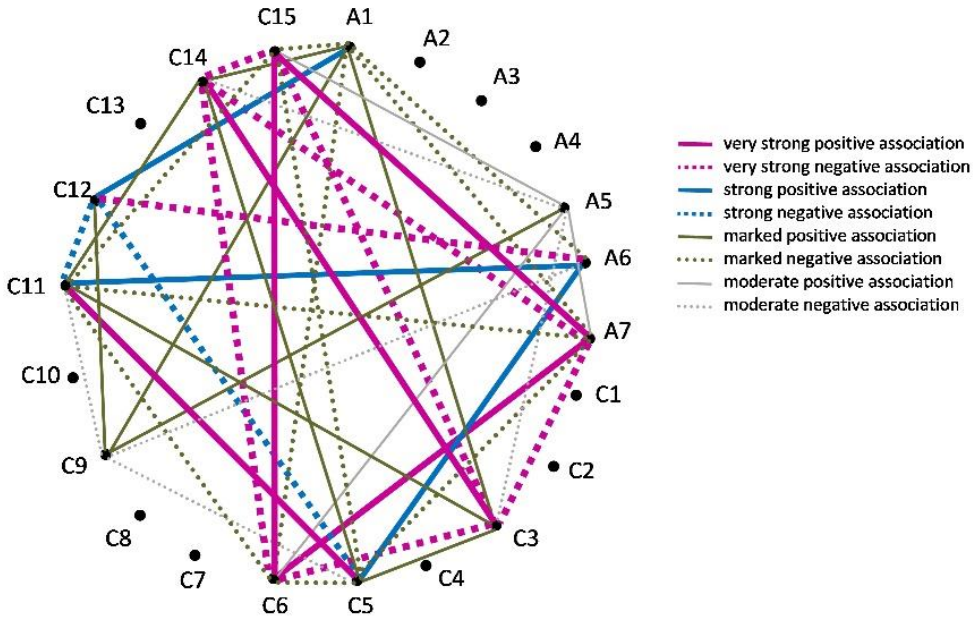

Figure 8. Correlation portrait of the morphofunctional basic capability of follicular cells under hyperthyroidism.

It is essential to note that follicular cells have evolved adaptive mechanisms to function under adverse conditions. We believe that signs of adaptation include very strong positive associations between cylindrical nuclei (C3) and narrow, unfragmented, highly dense marginal chromatin (C14), as well as between moderately wavy karyolemmata (C5) and dense central chromatin (C11). Negative associations of the same strength are also manifestations of adaptation. These associations are observed between the following: the cylindrical nuclei (C3) and the degeneratively altered lateral membranes (A7); a highly wavy karyolemmata (C6) and narrow, unfragmented, highly dense marginal chromatin (C14); between C14 and wide marginal chromatin (C15); and between unaltered lateral membranes (A6) and spotted central chromatin (C12).

Thus, hyperthyroidism is characterized by a complex configuration of correlations, including connections between signs of impaired hormone production, normal hormone production, and compensatory mechanisms. Functional disorders are characterized by connections between morphologically altered components of the profile, including cells of flattened shape and altered lateral membranes, as well as highly wavy karyolemmata, cylindrical nuclei, and lumpy and spotted central chromatin. The ability of follicular cells to function under hyperthyroid conditions is indicated by connections between morphologically unaltered components, such as moderately wavy karyolemmata and unaltered lateral membranes. The primary implementers of adaptive mechanisms are chromatin connections of varying degrees of condensation with other profile components.

4. Conclusions

The study of follicular cells under both normal and pathological conditions through the analysis of correlations between components of the morphofunctional basic capability profile significantly broadens and deepens the scope of scientific research. This approach enhances our understanding of the mutual influences and interdependencies among cellular components, thus contributing to the formation of objective knowledge about the follicular cell's activity as a cybernetic, self-regulating system.

An analysis of the relationships among components in the correlation portraits of follicular cells' morphofunctional basic capability revealed that, under thyroid homeostasis, specific correlations exist between the individual profile components. In the presence of functional disorders, these relationships may serve as the foundation for adaptive mechanisms. We refer to such correlations as "reserve" and believe they warrant further investigations.

When thyroid homeostasis is disturbed, the follicular cell activity proceeds through three concurrent processes: (1) functioning in accordance with existing pathological changes; (2) realization of compensatory and adaptive mechanisms; and (3) resolving functional disorders by establishing a new functional balance that allows continued normal operation.

The relationships between the components of the morphofunctional basic capability profile that provide mechanisms for the adaptation of follicular cells to adverse conditions (hypothyroidism, potentiated hypothyroidism, and hyperthyroidism) vary depending on the specific condition. Under iodine deficiency, the main functional load during follicular cell activity is borne by the cell and its nucleus. This is indicated by the characteristics of cuboidal and prism-shaped cells, whose central chromatin appears as fine-grained and sparse, while the marginal chromatin is either narrow or wide. In conditions of a potentiated iodine deficiency, adaptive mechanisms involve interactions between the following nuclear structures: a wavy karyolemma, fine-grained and sparse central chromatin, and

narrow, unfragmented marginal chromatin. Under hyperthyroid conditions, the primary adaptive mechanisms involve a connection between the cylindrical nucleus and dense central chromatin.

Author contributions

Olha Ryabukha conceived the work; served as the author and project leader of the study design; conducted the descriptive analysis of electron micrographs; created the database for correlation analysis; developed the idea of the graphical correlation portrait; described and interpreted the structure of the correlation portraits; drew conclusions; wrote the manuscript. Taras Lahotskyi performed the computations; created the correlation portraits; wrote subsection 2.2. Both authors approved the final version of the manuscript for publication.

Use of AI tools declaration

The authors declare that LanguageTool grammar-checking software was used.

Funding

This work was a fragment of the research projects carried out within the framework of the research topic “Improving the system of drug circulation during pharmacotherapy based on evidence-based and forensic pharmacy, organization, technology, biopharmacy, and pharmaceutical law”. Registered in the Ukrainian Institute of Scientific and Technical Expertise and Information of the Ministry of Education and Science of Ukraine (number 0120U105348, years of project implementation: 2021–2026).

Conflict of interest

The authors declare no conflict of interest.

References

1. Mendoza A, Hollenberg AN (2017) New insights into thyroid hormone action. *Pharmacol Ther* 173: 135–145. https://doi.org/10.1016/j.pharmthera.2017.02.012
2. Cicatiello AG, Di Girolamo D, Dentice M (2018) Metabolic effects of the intracellular regulation of thyroid hormone: old players, new concepts. *Front Endocrinol* (*Lausanne*) 11: 474. https://doi.org 10.3389/fendo.2018.00474
3. Patil N, Rehman A, Anastasopoulou C, et al. (2024) Hypothyroidism. Available from: https://www.ncbi.nlm.nih.gov/books/NBK519536/.
4. Feldt-Rasmussen U, Effraimidis G, Bliddal S, et al. (2024) Consequences of undertreatment of hypothyroidism. *Endocrine* 84: 301–308. https://doi.org/10.1007/s12020-023-03460-1
5. Chauhan A, Patel SS (2024) Thyroid hormone and diabetes mellitus interplay: Making management of comorbid disorders complicated. *Horm Metab Res* 56: 845–858. https://doi.org/10.1055/a-2374-8756

6. Mahmud T, Khan QU, Saad S (2021) The interplay between hyperthyroidism and ovarian cytoarchitecture in albino rats. *Cureus* 13: e14517. https://doi.org/10.7759/cureus.14517
7. LiVolsi VA, Baloch ZW (2018) The pathology of hyperthyroidism. *Front Endocrinol* (*Lausanne*) 9: 737. https://doi.org/10.3389/fendo.2018.00737
8. Editorial (2012) Thyroid disease – more research needed. *Lancet* 379: 1076. https://doi.org/10.1016/S0140-6736(12)60445-0
9. Taylor PN, Albrecht D, Scholz A, et al. (2018) Global epidemiology of hyperthyroidism and hypothyroidism. *Nat Rev Endocrinol* 14: 301–316. https://doi.org/10.1038/nrendo.2018.18
10. Moini J, Pereira K, Samsam M (2020) *Epidemiology of Thyroid Disorders*, Elsevier. https://doi.org/10.1016/C2018-0-03841-4
11. Zhang X, Wang X, Hu H, et al. (2023) Prevalence and trends of thyroid disease among adults, 1999–2018. *Endocr Pract* 29: 875–880. https://doi.org/10.1016/j.eprac.2023.08.006
12. Rossi ED, Tralongo P, Fiorentino V, et al. (2022) Approach to FNA of thyroid gland cysts. *Adv Anat Pathol* 29: 358–364. https://doi.org/10.1097/PAP.0000000000000357
13. Ghassabian A, Trasande L (2018) Disruption in thyroid signaling pathway: A mechanism for the effect of endocrine-disrupting chemicals on child neurodevelopment. *Front Endocrinol* 9: 204. https://doi.org/10.3389/fendo.2018.00204
14. Encarnação T, Pais AA, Campos MG, et al. (2019) Endocrine disrupting chemicals: Impact on human health, wildlife and the environment. *Sci Prog* 102: 3–42. https://doi.org/10.1177/0036850419826802
15. Burch HB (2019) Drug effects on the thyroid. *N Engl J Med* 381: 749–761. https://doi.org/10.1056/NEJMra1901214
16. Dietrich JW, Midgley JEM, Hoermann R (2018) Editorial: "Homeostasis and allostasis of thyroid function". *Front Endocrinol* 9: 287. https://doi.org/10.3389/fendo.2018.00287
17. Laurino A, Raimondi L (2022) Thyroid homeostasis: An intricate network of production, transport, metabolism and receptors interaction. *Int J Mol Sci* 23: 6751. https://doi.org/10.3390/ijms23126751
18. Pizzimenti C, Fiorentino V, Ieni A, et al. (2023) BRAF-AXL-PD-L1 signaling axis as a possible biological marker for RAI treatment in the thyroid cancer ATA intermediate risk category. *Int J Mol Sci* 24: 10024. https://doi.org/10.3390/ijms241210024
19. Ikramova SK (2025) Thyroid diseases as an important medical and social problem. *Am J Med Sci Pharm Res* 7: 85–88. https://doi.org/10.37547/tajmspr/Volume07Issue05-15
20. van Gerwen M, Alsen M, Little C, et al. (2020) Outcomes of patients with hypothyroidism and COVID-19: A retrospective cohort study. *Front Endocrinol* 11: 565. https://doi.org/10.3389/fendo.2020.00565
21. Shapovalova V (2022) Forensic and pharmaceutical risks in the organization of pharmacotherapy of covid, post-covid and long-covid disorders. COVID-19 and vaccination practice standards. *SSP Mod Pharm Med* 2: 1–24. https://doi.org/10.53933/sspmpm.v2i4.69
22. Shapovalova V (2022) An innovative multidisciplinary study of the availability of coronavirus vaccines in the world. *SSP Mod Pharm Med* 2: 1–17. https://doi.org/10.53933/sspmpm.v2i2.45
23. Karimova M, Shamansurova Z (2023) Thyroid status in patients after COVID19 in iodine deficiency region. *Endocr Abstr* 90: P503. https://doi.org/10.1530/endoabs.90.P503

24. Riabukha O (2015) Application of new information technologies for the study of cell activity, In: *Proceedings of the XIth International Conference on Perspective Technologies and Methods in MEMS Design*, 2–6, Lviv, Ukraine. New York (NY): IEEE, 69–71. Available from: https://ieeexplore.ieee.org/document/7299458.
25. Ryabukha O (2024) Theoretical and experimental approaches to study of biological objects by mathematical methods using the example of hormone production in the thyroid gland. *SSP Mod Pharm Med* 4: 1–14. https://doi.org/10.53933/sspmpm.v4i3.153
26. Wolff TM, Veil C, Dietrich JW, et al. (2022) Mathematical modeling and simulation of thyroid homeostasis: Implications for the Allan-Herndon-Dudley syndrome. *Front Endocrinol* 13: 882788. https://doi.org/10.3389/fendo.2022.882788
27. Fiorentino V, Pizzimenti C, Franchina M, et al. (2023) BRAF-AXL-PD-L1 signaling axis as a possible biological marker for RAI treatment in the thyroid cancer ATA intermediate risk category. *Diagn Histopathol* 29: 396–401. https://doi.org/10.1016/j.mpdhp.2023.06.013
28. von Bertalanffy L (1972) The history and status of General Systems Theory. *Acad Manag J* 15: 407–426. Available from: https://www.jstor.org/stable/255139.
29. Ryabukha O (2025) An innovative multidisciplinary approach to thyroid research: modern problems and solutions. *SSP Mod Pharm Med* 5: 13–29. https://doi.org/10.53933/mc22b767
30. Klyuchko OM (2018) Electronic expert systems for biology and medicine. *Biotechnol Acta* 11: 5–28. https://doi.org/10.15407/biotech11.06.005
31. Jones JH, Foster C (1942) A salt mixture for use with basal diets either low or high in phosphorus. *J Nutr* 24: 245–256. https://doi.org/10.1093/jn/24.3.245
32. Heald AH, Taylor P, Premawardhana L, et al. (2024) Natural desiccated thyroid for the treatment of hypothyroidism? *Front Endocrinol* (*Lausanne*) 8: 1309159. https://doi.org/10.3389/fendo.2023.1309159
33. Mikhailova TA (1963) The effect of thyroidin on the development of hypercholesteremia in sasting rabbits. *Bull Exp Biol Med* 54: 859–860. https://doi.org/10.1007/BF00787637
34. Petrovici A, Lupulescu A (1968) Ultrastructure of the normal thyroid gland, In: *Ultrastructure of the Thyroid Gland*, Basel: Karger, 4–34. https://doi.org/10.1159/000389735
35. Petrovici A, Lupulescu A (1968) Ultrastructural changes of the thyroid gland in different experimental conditions, In: *Ultrastructure of the Thyroid Gland*, Basel: Karger, 50–63. https://doi.org/10.1159/000389738
36. Ryabukha O (2023) Multidisciplinary studies of the thyroid gland's synthetic activity under conditions of iodine deficiency using correlation analysis. *SSP Mod Pharm Med* 3: 1–15. https://doi.org/10.53933/sspmpm.v3i3.104
37. Ryabukha O, Dronyuk I (2018) The portraits creating method by correlation analysis of hormone-producing cells data. *CEUR Workshop Proc* 2255: 135–145. Available from: http://ceur-ws.org/Vol-2255/paper13.pdf.
38. Patel A, Gupta S, Rehman Q, et al. (2013) Application of fuzzy logic in biomedical informatics. *J Emerg Trends Comput Inf Sci* 4: 57–62. Available from: https://api.semanticscholar.org/CorpusID:17783028.
39. Chaddock RE (1925) Interpretation of the coefficient of correlation, In: *Principles and Methods of Statistics*, Boston: Houghton Mifflin, 303–304. Available from: https://babel.hathitrust.org/cgi/pt?id=uc1.b3257183&view=1up&seq=323.

40. Caplan MJ (2016) Functional organization of the cell, In: Boron, W.F., Boulpaep, E.L., eds., *Medical Physiology*, 3rd Eds., Philadelphia: Elsevier, 8–46. Available from: https://shop.elsevier.com/books/medical-physiology/boron/978-1-4557-4377-3.
41. Barrett EJ, (2016) The Thyroid Gland, In: Boron, W.F., Boulpaep, E.L., eds., *Medical Physiology*, 3rd Eds., Philadelphia: Elsevier, 1006–1017. Available from: https://shop.elsevier.com/books/medical-physiology/boron/978-1-4557-4377-3.
42. American Medical Association (1969) Ultrastructure of the thyroid gland. *Arch Intern Med* 123: 111. https://doi.org/10.1001/archinte.1969.00300110113041